DOI: 10.1002/ejic.201100454

Electrostatic Interaction of Negatively Charged Core–Shell Nanoparticles with Antitumoral Cationic Platinum-Based Complexes

Miroslav Gál,[a,b] Ján Híveš,[c] Michele Laus,[b] Katia Sparnacci,[b] Mauro Ravera,[b] Elisabetta Gabano,[b] and Domenico Osella*[b]

Dedicated to Dr. Lubomir Pospíšil on the occasion of his 70th birthday

Keywords: Platinum / Antitumor agents / Nanoparticles / Electrochemistry / Electrostatic interactions

We report herein on the interaction between two cationic antiproliferative platinum compounds [namely *cis*-[PtCl-$(NH_3)_2$(py)]Cl (**1**) and *trans*,*trans*-[$(NH_3)_2$Pt{$NH_2(CH_2)_4NH_2$}-$PtCl(NH_3)_2$]$(Cl)_2$ (**2**)] and novel poly(methyl methacrylate) core–shell nanoparticles (MS) bearing anionic SO_3^- arms, studied to determine whether such particles might serve as drug carriers for Pt drugs. Electrostatic forces hold together the resulting adducts such that in the presence of higher concentrations of other cations the Pt drug should be released quickly and easily. As expected from their electric charges, we found that the formation constant of the MS-**2** adduct is significantly higher than that of MS-**1**. Moreover, the stability of both adducts depends on the ionic strength and surface charge density of competing cations in the medium. The stability of the conjugates and the consequent retention and release of the drug from the nanoparticles will thus depend on both blood and extracellular fluid composition.

Introduction

The discovery of the cytotoxic properties of *cis*-diamminedichloridoplatinum(II) (*cis*-$[PtCl_2(NH_3)_2]$, cisplatin) in the last century was a major breakthrough in the chemotherapeutic treatment of several solid tumors. The synthesis of new platinum complexes with a broader spectrum of antitumor activity and reduced systemic toxicity has been the main focus of research in medicinal inorganic chemistry in recent decades.[1] Despite this, only two complexes, carboplatin and oxaliplatin, have obtained worldwide approval for clinical use, with three other Pt compounds, namely nedaplatin (Japan), lobaplatin (China), and heptaplatin (South Korea), receiving only limited regional approval.[2]

The drug targeting and delivery approach aims at reducing chemotherapy-related systemic side-effects by using vectors to selectively convey the cytotoxic agents to tumor cells, thereby sparing healthy cells. In active targeting, the vectors can be bioactive substances, such as nutrients, that readily enter metabolically active tumor cells or they can be hormones, folates, or bile acids, which are selectively conveyed by receptors/transporters often overexpressed in cancer cells. Passive targeting, instead, uses naturally occurring or synthetically produced macromolecular vectors to exploit the so-called enhanced permeability and retention (EPR) effect[3] that results from the low vascularity, poor organization, and abnormal morphology of tumor vasculature. The vascular endothelium in tumors proliferates rapidly and is intrinsically discontinuous because it has a higher number of fenestrations and open junctions than normal vessels.[4] Moreover, the lack of a functional lymphatic network prevents efficient removal of excess fluid from solid tumor tissue.[5] The combination of these two effects makes tumors hyperpermeable to circulating macromolecules, which extravasate and accumulate in the extratumoral tissue where they are retained for long periods.[6]

Over the past few decades, polymer therapeutics have emerged as an important facet of nanomedicine.[7] This term includes polymer–drug conjugates[8] in which a bioactive molecule is covalently linked to a polymeric vector. The particular relevance of these studies to the area of antitumoral Pt-based complexes is testified by the number of conjugates now finding acceptance as a new class of antitumor agents.[9] In particular, two conjugates developed by Access Pharmaceuticals have reached clinical trials. AP5280 consists of a cisplatin-like Pt–diammine unit linked to the water-soluble, biocompatible co-polymer HPMA [HPMA = *N*-(2-hydroxypropyl)methacrylamide].[10] The platinum

[a] J. Heyrovský Institute of Physical Chemistry, Academy of Sciences of the Czech Republic, v.v.i.,
Dolejškova 3, 182 23 Prague 8, Czech Republic
[b] Dipartimento di Scienze dell'Ambiente e della Vita, Università del Piemonte Orientale "A. Avogadro",
Viale T. Michel 11, 15121 Alessandria, Italy
Fax: +39-0131-360250
E-mail: domenico.osella@mfn.unipmn.it
[c] Faculty of Chemical and Food Technology, Slovak Technical University Bratislava,
Radlinského 9, 81237 Bratislava, Slovak Republic

moiety is linked as an *N*,*O*-chelate through an amidomalonic group at the distal end of a thiol-dependent protease-cleavable tetrapeptide linker, Gly-Phe-Leu-Gly. AP5280 is active against lung, ovarian, head, and neck cancer as well as melanoma.[11] AP5346 (ProLindac™) is structurally similar to AP5280 but with 1*R*,2*R*-diaminocyclohexane as the carrier group instead of two NH_3 moieties and the amidomalonic chelating group is linked to the polymer backbone through the tripeptide Gly-Gly-Gly.[12] This conjugate has completed Phase II clinical trials and shows enhanced selectivity for tumor tissue, favorable toxicity profiles,[13] and activity against malignities that do not respond to treatment with standard Pt drugs.

In this context, lipoplatin™ and lipoxal™ (nanoparticles composed of lipids and cisplatin or oxaliplatin, respectively) are worthy of mention because these candidate drugs show less side-effects with respect to the free complex for the majority of treated adenocarcinomas.

An alternative to the use of a hydrolyzable or enzymatically degradable group is to build up conjugates through electrostatic interactions. A host of functional nanospheres of submicron size with cationic surface groups, designed specifically for the reversible adsorption of anionic bioactive species, have been prepared by emulsion polymerization with methyl methacrylate as the monomer and a cationic co-monomer as the emulsion stabilizer.[14] At the end of the reaction, the water-soluble units deriving from the cationic monomer are preferentially located at the nanosphere surface, which can thus be tailored to the chemical structure of the co-monomer employed.

The latter approach was taken in a recent study that used poly(methyl methacrylate) (PMMA) core–shell nanospheres (ZN2), bearing positively charged ammonium arms, as vectors for the anionic amminetrichloridoplatinum complex (PtA). It has previously been reported that these nanospheres do not interfere with the proliferation of primary HL60 as well as PBMC cells up to a concentration of 100 mg mL^{-1}.[15]

The antitumor effect of the resulting adduct PtA–ZN2 was assessed in C57BL/6 mice bearing B16 murine melanoma. When used at the corresponding maximum tolerated doses, PtA–ZN2 proved far more effective than cisplatin in inhibiting B16 tumor growth. As expected, the in vivo efficacy of PtA–ZN2, cisplatin, and PtA correlated with Pt intratumor accumulation.[16] Although the PtA released from PtA–ZN2 is inherently less potent than cisplatin (ca. 20 times less), it still afforded a significant benefit when administered in vivo as a polymer conjugate. Spectrophotometric measurements of the thiopeptolide substrate concentration indicate that PtA also inhibits the matrix metalloproteinase MMP-3 involved in cancer progression.[17] This has been confirmed by tests on the matrigel invasion of selected cell lines,[18] a prerequisite for demonstrating the antimetastatic propensity of drug candidates.

This work adopts a similar strategy for the design and synthesis of novel PMMA core–shell nanoparticles bearing negatively charged SO_3^- arms (MS, Figure 1) conjugated to cationic Pt complexes.

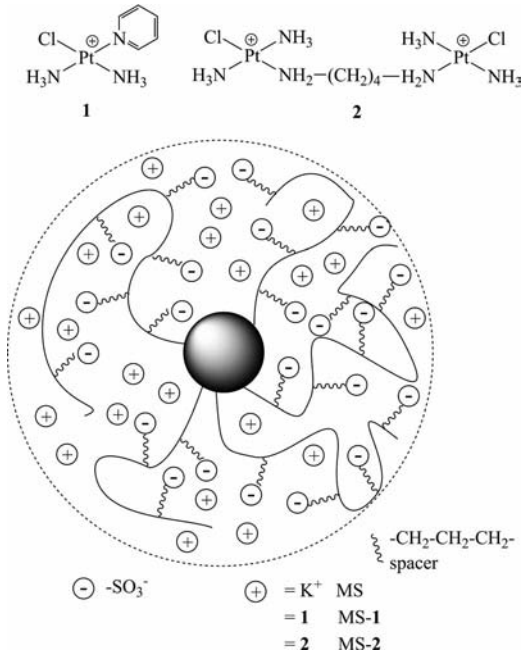

Figure 1. Structures of complexes **1** and **2** and their conjugates with MS nanospheres.

For this purpose, two cationic Pt complexes with remarkable antiproliferative activity were selected. The first, the cationic *cis*-[PtCl(NH_3)$_2$(py)]Cl (**1**), is active against colorectal cancers overexpressing organic cation transporters.[19] The second, the dicationic *trans,trans*-[Cl(NH_3)$_2$Pt{NH_2-(CH_2)$_4$$NH_2$}PtCl($NH_3$)$_2$](Cl)$_2$ (**2**),[20] forms adducts that are different to those of cisplatin and can thus overcome both natural and acquired drug resistance.

Ionic interactions in aqueous medium between the two positively charged platinum drug candidates **1** and **2** and the negatively charged nanospheres MS lead to the conjugates MS-**1** and MS-**2**, respectively.

We used electrochemical techniques to assess the stability of the MS-**1** and MS-**2** adducts and to study the release of Pt complexes **1** and **2** under different experimental conditions. Because the shifts of the reduction potentials of the adducts MS-**1** and MS-**2** relative to the free Pt complexes **1** and **2**, respectively, could be determined directly with no interference effect, we were able to determine the stability of the resulting adducts under several experimental conditions.[21]

Results and Discussion

The core–shell nanosphere MS was prepared by emulsion polymerization of methyl methacrylate in the presence of an anionic co-monomer, namely the 3-sulfopropyl methacrylate potassium salt. Similar polymerization systems lacking regular emulsifiers are well known and essentially involve one reactive component, the "surfmer" or "polymerizable surfactant", which serves to stabilize the emulsion. As reported for many emulsion polymerization systems that include water-soluble co-monomers, the reaction

starts in the aqueous phase leading to the formation of water-soluble oligoradicals that are rich in the water-soluble co-monomer until they reach the limit of solubility and precipitate to form primary particles, which are able to grow by the incorporation of monomer and co-monomer. The water-soluble units are preferentially located at the nanosphere surface and actively participate in latex stabilization. Nanospheres can thus be obtained with tailored surfaces dictated by the chemical structure of the co-monomer employed, ultimately leading to the formation of core–shell nanospheres. In particular, the formation of a highly hydrophilic shell can be envisaged in which the various arms, protruding from the core to the water phase, provide functional centers suitable for ionic interaction with the bioactive complex.

Nanoparticles MS are characterized by an average SEM diameter of 165 ± 70 nm (Figure 2) and by a hydrodynamic diameter, evaluated by dynamic light scattering (DLS), of 210 nm. The amount of negatively charged groups available for interaction with the platinum complex was obtained by determination of the sulfur content by elemental analysis and turned out to be 0.45 ± 0.03% (w/w), which corresponds to 140 ± 9 μmol of SO_3^- groups per gram of nanoparticles.

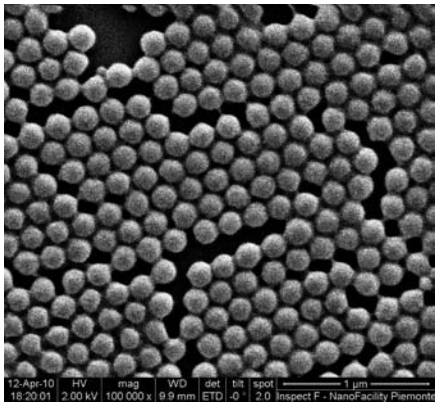

Figure 2. SEM image of MS core–shell nanoparticles.

The ability of core–shell nanoparticles MS to interact with platinum complexes **1** and **2** to form supramolecular adducts MS-**1** and MS-**2** was studied electrochemically. Cyclic voltammetry (CV), direct current (DC) tast polarography, and differential pulse polarography or voltammetry (DPP/DPV) were employed to obtain the formation constants K of the adducts in aqueous solutions of different ionic strength.

The DC tast polarograms of **1** and **2** in 0.1 M NaCl are shown in Figure 3. In the low potential region at around –200 (**1**) and –300 mV (**2**) versus the reference electrode (RE) one polarographic wave for each free complex is clearly visible. These waves are assigned to the $Pt^{II} \rightarrow Pt^0$ reduction process. The reduction potentials of **1** and **2** are in the range found for similar Pt compounds.[22] The height of the reduction wave of **2** is about twice that of **1**, as expected from the stoichiometry of the complex, provided that the two electroactive Pt centers are reduced independently.[23] In the very negative potential region at around –1420 mV versus RE, one catalytic peak on the DC polarogram is observed for both compounds (catalytic hydrogen evolution, not shown in Figure 3).

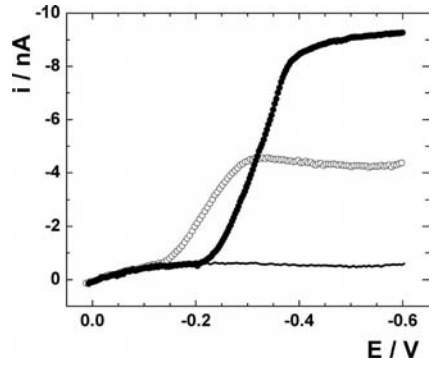

Figure 3. DC tast polarograms of **1** (○) and **2** (●) obtained by using 0.1 M NaCl as the supporting electrolyte. c(**1**) = 1.97×10^{-6} M, c(**2**) = 2.01×10^{-6} M. The flat line at the bottom is the background current.

The polarographic response of complex **1** in the presence of increasing amounts of core–shell MS nanoparticles is presented in Figure 4. The interaction of **2** with MS produced similar results.

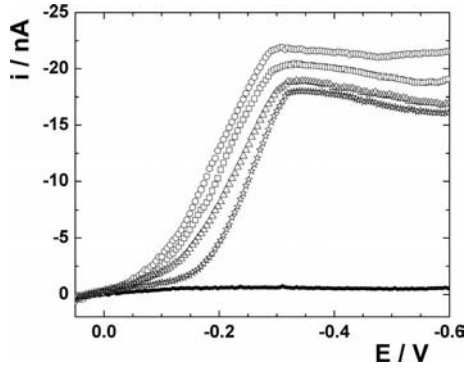

Figure 4. DC tast polarograms of an aqueous solution of 8.70×10^{-6} M of **1** and 0.1 M of the supporting electrolyte NaCl with different amounts of MS added. The concentration of MS is expressed as the molarity of the corresponding sulfonic groups: (○) 0.00 M; (□) 3.40×10^{-5} M; (Δ) 8.90×10^{-5} M; (☆) 6.30×10^{-4} M SO_3H^-. Flat line at the bottom is the background current.

The interaction of **1** with nanoparticles MS causes a shift of the reduction potential towards more negative values as well as a decrease in the polarographic wave (limiting current). The decreasing height of the polarographic curve corresponds to the enhancement of the apparent diffusion coefficient of the MS-**1** adduct with respect to free complex **1**.[24] Several electrochemical tests were performed to check that the decrease in the reduction wave of **1** following the addition of MS was due neither to increased viscosity of the solution nor to contamination of the electrode surface by an adsorbed layer of MS.

Figure 5 shows the shift of the half-wave potential $E_{1/2}$ for the reduction of **1** in 0.1 M NaCl with an increasing amount of MS (expressed as the molar concentration of the

corresponding sulfonate groups). The experimental points can be fitted by an exponential decay curve, which implies that the shift of $E_{1/2}$ is most significant after the addition of the first portions of MS to the solution of **1**: Only some of the SO_3H^- groups (likely those on the outer shell) of the MS nanoparticles are able to form adducts with **1**.

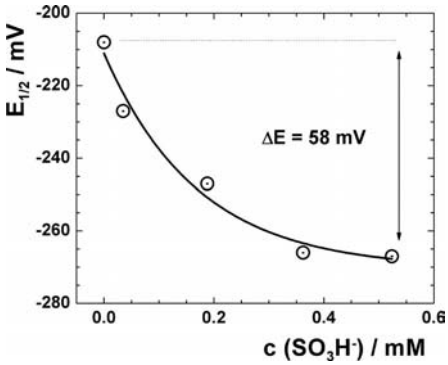

Figure 5. Exponential decay fit (− −) of the experimental half-wave reduction potential shifts (⊙) of **1** after the addition of various amounts of MS in 0.1 M NaCl. c(**1**) = 1.19×10^{-5} M.

Similar behavior was observed for the MS-**2** system (Figure 6). The shift of the reduction potential of the MS-**2** adduct compared with the free compound **2** (91 mV, Figure 6) is higher than the shift of MS-**1** compared with **1** (58 mV, Figure 5), which indicates a higher stability of the former with respect to the latter. It is likely that the two positive Pt moieties in **2** can link either two different anions in the same nanoparticle (intramolecular interaction) or two different anions of two different MS nanoparticles (intermolecular interaction). The occurrence of intermolecular cross-linking interactions brought about by the diplatinum cation **2** causes aggregation of the nanoparticles at a high **2**/MS stoichiometric ratio. The precedent of DNA aggregation caused by similar positively charged polyplatinum cations has been reported.[25]

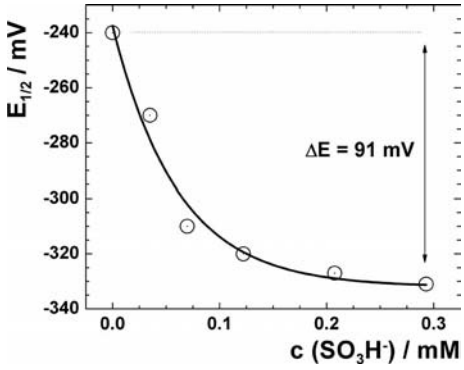

Figure 6. Exponential decay fit (− −) of the experimental half-wave reduction potential shifts (⊙) of **2** after the addition of various amounts of MS in 0.1 M NaCl [c(**2**) = 8.90×10^{-6} M].

The Lingane approach was used to estimate and compare the stability of the MS-**1** and MS-**2** conjugates in the various supporting electrolytes.[26] The reduction potential of free metal ions is strongly affected by the presence of suitable ligands (especially chelating ligands) and the $E_{1/2}$ (as well as peak potential) value of the resulting complex is shifted to a more negative potential (i.e., a higher energy is necessary to reduce metal ions in the complexes than free metal ions). Accordingly, the half-wave potential shift $\Delta E_{1/2}$ can be used to determine the complex formation constant K.[21] Lingane derived Equation (1) for the half-wave potential shift $\Delta E_{1/2}$[26] in which n is the number of electrons transferred during the reduction reaction, p is the ligand/metal-ion molar ratio, K is the complex formation constant, and c_L is the concentration of the ligand. The adduct formation constants are reported in Table 1.

$$\Delta E_{1/2} \cong \frac{0.0591}{n} \log K - 0.0591 \frac{p}{n} \log c_L \quad (1)$$

Table 1. Complex formation constants K for MS-**1** and MS-**2** complexes in various solutions.

Electrolyte	K [L mol^{-1}]	
	MS-**1**	MS-**2**
0.005 M LiCl	1.29×10^2	9.77×10^3
0.1 M LiCl	5.02×10^0	1.88×10^1
0.005 M NaCl	8.98×10^4	6.91×10^5
0.1 M NaCl	2.40×10^2	5.13×10^3
0.154 M NaCl	1.80×10^2	4.72×10^4
0.005 M KCl	1.12×10^5	2.48×10^7
0.1 M KCl	5.56×10^3	9.07×10^5
0.005 M NH_4Cl	6.17×10^6	2.55×10^8
0.1 M NH_4Cl	1.53×10^4	1.36×10^6

The adduct MS-**2** is more stable than MS-**1** under all the experimental conditions. The conjugates become less stable with increasing concentration of the supporting electrolyte, which contains monocations able to compete with the positively charged Pt complexes **1** and **2** for the ionic interaction with the sulfonate groups. The bulkier the competing monocation, the greater the stability of the MS-**1** and MS-**2** adducts in the presence of the supporting electrolyte. This is in agreement with previous observations.[27]

The dependence of the log K values of the adducts MS-**1** and MS-**2** on the electron affinities E_{EA} of the competing monocations[28] in the supporting electrolyte is shown in Figure 7. The higher the electron affinity of the competing

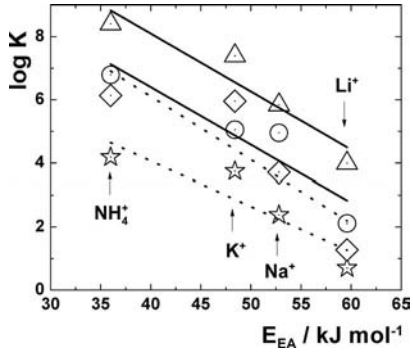

Figure 7. Dependence of electron affinity E_{EA} on log K for both solution concentrations and for all ions: (Δ) **2** in 0.005 M solution; (⊙) **1** in 0.005 M solution; (◇) **2** in 0.1 M solutions; (☆) **1** in 0.1 M solutions. E_{EA} values taken from ref.[28]

cation, the less stable the adducts. It was found that the competing ability follows the Hofmeister series ($NH_4^+ < K^+ < Na^+ < Li^+$). By comparing the data in Table 1, one can conclude that the cationic Pt complexes **1** and **2** are more affined to MS nanospheres than the simple cations (NH_4^+, K^+, Na^+, Li^+) of the supporting electrolyte employed. However, if the concentration of these cations is high, **1** and **2** are inevitably released from the nanosphere conjugates. These observations fit with those made by Salis et al.[27]

A similar approach has also been applied to *p*-sulfonatocalix[4]arenes, used as drug delivery vehicles for multinuclear Pt anticancer drugs in which ionic interaction reinforces encapsulation.[29]

Conclusions

Our results show that nanospheres bearing charged arms can form conjugates through ionic interactions with oppositely charged antiproliferative Pt complexes **1** and **2** and may therefore be potential carriers for this type of drug. Importantly, the cationic Pt complexes are more affined to MS nanospheres than the simple cations NH_4^+, K^+, Na^+, and Li^+. When the concentration of competing cations is high (i.e., salts naturally present in the biological milieu, such as in blood or the extracellular matrix), **1** and **2** are released from the nanosphere conjugates assuring the necessary delivery of the drug. Tests on the controlled release of Pt complexes **1** and **2** from adducts MS-**1** and MS-**2** under physiological conditions are in progress.

Experimental Section

All chemicals were analytical grade and were obtained from Aldrich (except for $K_2[PtCl_4]$, which was from Alfa Aesar) and used as received. Complexes **1**[30] and **2**[31] were prepared according to standard procedures. Elemental analyses were carried out with an EA3000 CHN Elemental Analyzer (EuroVector, Milano, Italy). Platinum was quantified by means of a Spectro Genesis ICP-OES spectrometer (Spectro Analytical Instruments, Kleve, Germany) equipped with a cross-flow nebulizer. To quantify the platinum concentration the Pt 299.797 line was selected. A platinum standard stock solution of 1000 mg L^{-1} was diluted in 1.0% v/v nitric acid to prepare calibration standards. The elemental analyses and Pt content were within ±0.4% absolute of the theoretical value. The multinuclear NMR spectra were measured with a JEOL Eclipse Plus spectrometer operating at 400 (^{1}H), 100.5 (^{13}C), and 85.9 MHz (^{195}Pt with a spectral window of 1200 ppm), respectively. ^{1}H and ^{13}C NMR chemical shifts were reported in parts per million referenced to solvent resonances. ^{195}Pt NMR spectra were recorded using a solution of $K_2[PtCl_4]$ in saturated aqueous KCl as external reference. The shift for $K_2[PtCl_4]$ was adjusted to –1628 ppm relative to that of $Na_2[PtCl_6]$ (δ = 0 ppm). Electrospray mass spectra (ESI-MS) were obtained by using a Micromass ZMD mass spectrometer. Typically, a dilute solution of the compound was delivered directly to the spectrometer source at 0.01 mL min^{-1} using a Hamilton microsyringe controlled by a single-syringe infusion pump. The nebulizer tip operated at 3000–3500 V and 150 °C with nitrogen used both as a drying and a nebulizing gas. The cone voltage was 30 V. Quasi-molecular ion peaks $[M + H]^+$ or sodiated $[M + Na]^+$ peaks were assigned on the basis of the *m*/*z* values and of the simulated isotope distribution patterns.

Electrochemical measurements were performed by using an AUTOLAB PGSTAT12 instrument (ECO Chemie, The Netherlands). Electrochemical data were analyzed by using ORIGIN® software. A three-electrode electrochemical cell was used. The reference electrode (RE), Ag|AgCl|3 M KCl, was separated from the test solution by a salt bridge. The working electrode (WE) was a valve-operated static mercury electrode (VA Stand 663, Metrohm). The counter electrode (CE) was a cylindrical platinum rod with an area around 100 times that of the WE. Oxygen was removed from freshly prepared solutions of **1** or **2** and MS by purging and stirring for about 20 min with nitrogen prior to each experiment.

Synthesis and Characterization of the Negatively Charged PMMA Core–Shell Nanoparticles: The negatively charged PMMA core–shell nanoparticles were prepared by emulsion polymerization of methyl methacrylate in the presence of the ionic co-monomer 3-sulfopropyl methacrylate potassium salt as the emulsion stabilizer.

An aqueous solution (500 mL) of 3-sulfopropyl methacrylate potassium salt (5.6 g, 22.8 mmol) was introduced at room temperature into a 1 L five-necked reactor equipped with a condenser, a mechanical stirrer, a thermometer, and inlets for nitrogen. The mixture was purged with nitrogen at a stirring rate of 300 rpm and heated to 80 °C, after which methyl methacrylate (65.50 g, 655 mmol) was added. After another 15 min equilibration time, potassium persulfate (170 mg, 0.630 mmol) dissolved in deionized water (5 mL) was added and the mixture was allowed to react for 4 h. At the end of the reaction, the product was purified by dialysis to remove residual monomer and stabilizer.

The size and size distribution of the nanospheres were measured with a JEOL JSM-35CF scanning electron microscope (SEM) with an accelerating voltage of 20 kV. Samples were sputter-coated under vacuum with a thin layer (10–30 Å) of gold. The SEM micrograph was elaborated using the ImageJ (version 1.44, public domain) image processing software. The diameters of 150–200 individual nanospheres were measured and were determined to be 165 ± 7 nm. The sulfur content was determined by elemental analysis, TGA, and volumetric methods. The average amount proved to be 0.45 ± 0.03% (w/w), which corresponds to 140 ± 9 μmol g^{-1} SO_3^- groups.

Acknowledgments

This study received financial support from the Regione Piemonte (a grant to M. G. within the Research Project "Biosensors for environmental and pharmaceutical applications") and the Grant Agency of the Czech Republic (203/09/P502) and was carried out within the auspices of the International Cooperation Agreement between the J. Heyrovsky Institute (Prague) and the Dipartimento di Scienze dell'Ambiente e della Vita (DiSAV, Alessandria).

[1] M. Galanski, M. A. Jakupec, B. K. Keppler, *Curr. Med. Chem.* **2005**, *12*, 2075–2094.
[2] N. J. Wheate, S. Walker, G. E. Craig, R. Oun, *Dalton Trans.* **2010**, *39*, 8113–8127.
[3] a) Y. Matsumura, H. Maeda, *Cancer Res.* **1986**, *46*, 6387–6392; b) H. Maeda, J. Wu, T. Sawa, Y. Matsumura, K. Hori, *J. Controlled Release* **2000**, *65*, 271–284.
[4] D. F. Baban, L. W. Seymour, *Adv. Drug Delivery Rev.* **1998**, *34*, 109–119.

[5] A. J. Leu, D. A. Berk, A. Lymboussaki, K. Alitalo, R. K. Jain, *Cancer Res.* **2000**, *60*, 4324–4327.
[6] H. Maeda in *Biomedical Aspects of Drug Targeting* (Eds.: V. Muzykantov, V. P. Torchilin), Kluwer, Dordrecht, **2003**, pp. 211–229.
[7] R. Duncan, *Nat. Rev. Drug Discovery* **2003**, *2*, 347–360.
[8] R. Duncan, *Nat. Rev. Cancer* **2006**, *6*, 688–701.
[9] a) B. Twaites, C. de las Heras Alarcòn, C. Alexander, *J. Mater. Chem.* **2005**, *15*, 441–455; b) W. H. Mandeville, D. I. Goldberg, *Curr. Pharm. Des.* **1997**, *3*, 15–28.
[10] D. R. Stewart, J. R. Rice, J. V. St. John, US Pat. 6692734.
[11] a) M. Bouma, B. Nuijen, D. R. Stewart, J. R. Rice, B. A. Jansen, J. Reedijk, A. Bult, J. H. Beijnen, *Anti-Cancer Drugs* **2002**, *13*, 915–924; b) M. Bouma, B. Nuijen, R. Harms, D. P. Nowotnik, D. R. Stewart, B. A. J. Jansen, S. van Zutphen, J. Reedijk, M. J. van Steenbergen, H. Talsma, A. Bult, J. H. Beijnen, *Drug Dev. Ind. Pharm.* **2003**, *29*, 981–995; c) X. Lin, Q. Zhang, J. R. Rice, D. R. Stewart, D. P. Nowotnik, S. B. Howell, *Eur. J. Cancer* **2004**, *40*, 291–297.
[12] P. Sood, K. B. Thurmond, J. E. Jacob, L. K. Waller, G. O. Silva, D. R. Stewart, D. P. Nowotnik, *Bioconjugate Chem.* **2006**, *17*, 1270–1279.
[13] J. R. Rice, J. L. Gerberich, D. P. Nowotnik, S. B. Howell, *Clin. Cancer Res.* **2006**, *12*, 2248–2254.
[14] K. Sparnacci, L. Tondelli, M. Laus, *J. Polym. Sci., Part A: Polym. Chem.* **2000**, *38*, 3347–3354.
[15] a) L. Tondelli, A. Ricca, G. Citro, M. Lelli, M. Laus, *Nucleic Acids Res.* **1998**, *26*, 5425–5431; b) L. Tondelli, E. Canto, A. Pistagna, S. Buttò, A. Tripiciano, R. Cortesi, K. Sparnacci, M. Laus, *J. Biomater. Sci., Polym. Ed.* **2001**, *12*, 1339–1357.
[16] E. Monti, M. B. Gariboldi, R. Ravizza, R. Molteni, K. Sparnacci, M. Laus, E. Gabano, M. Ravera, D. Osella, *Inorg. Chim. Acta* **2009**, *362*, 4099–4109.
[17] F. Arnesano, A. Boccarelli, D. Cornacchia, F. Nushi, R. Sasanelli, M. Coluccia, G. Natile, *J. Med. Chem.* **2009**, *52*, 7847–7855.
[18] D. Osella, E. Ranzato, unpublished work.
[19] K. S. Lovejoy, R. C. Todd, S. Zhang, M. S. McCormick, J. A. D′Aquino, J. T. Reardon, A. Sancar, K. M. Giacomini, S. J. Lippard, *Proc. Natl. Acad. Sci. USA* **2008**, *105*, 8902–8907.
[20] N. Farrell in *Platinum-Based Drugs in Cancer Therapy* (Eds.: L. R. Kelland, N. Farrell), Humana Press, Totowa, NJ, **2000**, pp. 321–338.
[21] T. Caykara, R. Inam, Z. Ozturk, O. Guven, *Colloid Polym. Sci.* **2004**, *282*, 1282–1285.
[22] J. Heyrovský, J. Kůta, *Principles of Polarography*, Academic Press, New York, **1966**.
[23] A. J. Bard, L. R. Faulkner, *Electrochemical Methods: Fundamentals and Applications*, 2nd ed., **1980**, Wiley, New York.
[24] D. H. Evans, *J. Electroanal. Chem.* **1989**, *258*, 451–456.
[25] T. Banerjee, P. Dubey, R. Mukhopadhyay, *Biochimie* **2010**, *92*, 846–851.
[26] J. J. Lingane, *Chem. Rev.* **1941**, *29*, 1–35.
[27] A. Salis, D. F. Parsons, M. Bostrom, L. Medda, B. Barse, B. W. Ninham, M. Monduzzi, *Langmuir* **2010**, *26*, 2484–2490.
[28] a) T. S. Almeida, K. Coutinho, B. J. C. Cabral, S. Canuto, *J. Chem. Phys.* **2008**, *128*, 014506; b) C. Nordling, J. Österman, *Physics Handbook for Science and Engineering*, 8th ed., Studentlitteratur, Lund, **2006**.
[29] N. J. Wheate, G. M. Abbott, R. J. Tate, C. J. Clements, R. Edrada-Ebel, B. F. Johnston, *J. Inorg. Biochem.* **2009**, *103*, 448–454.
[30] M. Valsecchi, M. Conti, L. Del Greco, C. Bugatti, E. Menta, F. Giuliani, C. Manzotti, S. Spinelli, N. Farrell, US Pat. 5744497.
[31] L. S. Hollis, A. R. Amundsen, E. W. Stern, *J. Med. Chem.* **1989**, *32*, 128–136.

Received: April 28, 2011
Published Online: ■

